Adsorption and Photodegradation of Dimethyl Methylphosphonate Vapor at TiO_2 Surfaces

John A. Moss, Steven H. Szczepankiewicz,† Eleanor Park, and Michael R. Hoffmann*

W. M. Keck Laboratories, California Institute of Technology, Pasadena, California 91125

Received: April 20, 2005; In Final Form: July 11, 2005

The adsorption and degradation of the nerve agent simulant dimethyl methylphosphonate (DMMP) over UV-irradiated TiO_2 powders and thin films has been investigated. Adsorption of vapor-phase DMMP on TiO_2 powder is characterized by diffuse reflectance infrared Fourier transform spectroscopy (DRIFTS). Photochemically assisted oxidation of adsorbed DMMP is carried out in situ by irradiation of samples in the DRIFTS accessory, giving kinetic data and information on specific site binding of DMMP and catalyst poisoning. Gas-phase intermediates from a static vapor phase reaction are identified by gas chromatography−mass spectrometry analysis, and surface-bound intermediates and products are analyzed by high-performance liquid chromatography−mass spectrometry, and ion chromatography of both aqueous and organic extractions from the TiO_2. Adsorbed DMMP is photodegraded in a stepwise fashion to give methylphosphonic acid, PO_4^{3-}, H_2O, and CO_2 as products. A proposed reaction pathway is consistent with a rapid degradation of DMMP but with extensive poisoning of the catalyst by surface-bound phosphonate products.

Introduction

Current gas-mask technology and larger ambient air filtration methods for the capture and destruction of chemical nerve agent vapors involves trapping the contaminant in a carbon bed followed by a separate chemical decontamination step involving hydrolysis or chemical oxidation, Heterogeneous strategies employ reactive surfaces, such as metal oxides, to capture and degrade the contaminants to benign gas-phase and surface-bound products. The applicability of this method is largely determined by the surface chemistry of the organophosphorus compound and the properties of the reactive surface, which may depend greatly on the environmental conditions and surface preparation.

Of particular interest has been the adsorption and decomposition of organophosphonate compounds on metal or metal oxide surfaces.[1] The specific adsorption of dimethyl methylphosphonate (DMMP), a simulant for organophosphorus nerve agents such as Sarin or VX has been investigated on supported metal catalysts (Pt/Al_2O_3),[2−4] single-crystal metals (Rh(100),[5] Ni(111),[6] Pd(111),[6] and Mo(110),[7] and oxides[8] (Al_2O_3,[9,10] SiO_2,[11] α-Fe_2O_3,[11,12] MgO,[13−16] AMO,[17] and others). These surfaces degrade DMMP either catalytically or stoichiometrically by dealkylation, hydrolysis, or oxidation to give desorbable small-molecule products and surface-bound phosphates. The high surface area of the oxide materials provides a large adsorption capacity, allowing subsequent thermal destruction of the captured contaminants. The mode of DMMP binding to the surface and the mechanism of reaction have been investigated in these systems by Fourier transform infrared spectroscopy (FTIR), high-resolution electron energy loss spectroscopy (HREELS), secondary ion mass spectrometry (SIMS), thermal programmed desorption, Auger electron spectroscopy, and other techniques.

An alternative strategy is to employ the high surface area of a metal oxide for contaminant adsorption, but with photocatalytic degradation of the substrate. Titanium dioxide has been shown to be an effective photocatalyst for the degradation of a large number of organic and inorganic compounds in both aqueous solution[18−20] and the gas phase.[21−24] For organophosphorus compounds, namely DMMP, a number of studies have examined the reaction of gas-phase DMMP with TiO_2 or the DMMP−TiO_2 surface interaction. Obee and Satyapal investigated intrinsic rates, products, and catalyst poisoning for DMMP photodegradation in a single-pass reactor.[25] An additional report detailed the IR spectra of DMMP adsorbed on TiO_2 but found no evidence for photodegradation.[26] Recently, Rusu and Yates have extensively investigated the adsorption[27] and photooxidation[28] of DMMP on TiO_2 powder. They identified three regions of adsorptive behavior: a condensation region below 160 K, a diffusion region from 160 to 200 K where condensed DMMP diffused to the TiO_2 particle interior and undergoes H-bonding to isolated TiOH groups, and a decomposition region above 214 K where P−OCH_3 is cleaved thermally. They also studied the photooxidation process at 200 K, identifying adsorbed reaction products.

Here we investigate the adsorption and photocatalytic degradation of DMMP vapor at room temperature on Degussa P-25 TiO_2 powders by diffuse reflectance Fourier transform infrared spectroscopy (DRIFTS). DRIFT spectroscopy is an ideal technique for examining the interaction of gas- or vapor-phase compounds with TiO_2 for several reasons. DRIFTS is relatively simple and inexpensive compared to other surface techniques such as X-ray photoelectron spectroscopy (XPS) and HREELS. Bulk materials may be examined in their native state as powders or films without special preparation such as adsorption on sample grids. Finally, DRIFTS provides functional group information (e.g., alkyl vs alkoxy) for elucidation of mechanistic details and inhibitory effect of intermediates and products on subsequent degradations, and these details are available for both the adsorbent and adsorbate. In the study reported here, vapor-phase DMMP is adsorbed onto TiO_2 powder, and both the adsorption and subsequent photocatalytic decomposition of the adsorbed DMMP may be followed by DRIFTS. These results

* To whom correspondence should be addressed. E-mail: mrh@its.caltech.edu. Phone: (626) 395-4391. FAX: (626) 395-2940.

† Present address: Department of Chemistry, Canisius College, Buffalo, NY 14208.

10.1021/jp052057j CCC: $30.25
Published on Web 10/05/2005

are compared to those from batch photochemical reactions on bulk TiO_2 powder and TiO_2 films, with an aim for understanding the background surface chemistry necessary for developing photocatalytic filter devices for the removal of chemical warfare agents from air.

Experimental Methods

Materials. Polycrystalline TiO_2 (Degussa P-25) and fumed silica (SiO_2) (Aldrich, 14 nm particle size) were purified by sonication in deionized water and recovered by ultracentrifugation before being dried under vacuum. Dimethyl methylphosphonate (DMMP) and methylphosphonic acid (MPA) were obtained from Aldrich and used as received. All chemicals were reagent grade or better and used as received. O_2 was dried by passing through a P_2O_5 column. N_2 was purified by passing through $CaCl_2$, P_2O_5, and an Oxy-Trap column. Kinetic simulation was performed with the package KinTekSim (KinTec Corp., State College, PA; http://www.kintek-corp.com).[29,30]

Instrumental Methods. Gas chromatography−mass spectrometry (GC−MS) was carried out with a HP 5890 GC and HP 5989A mass-selective detector using either a 25 m length × 0.32 mm diameter × 0.52 μm thickness HP−FFAP column (DMMP and other organophosphonates) or a 30 m length × 0.25 mm diameter × 1.0 μm thickness HP-5MS column (CH_3-OH, HCOOH, HCHO, and CO_2). Liquid chromatography−mass spectrometry (LC-MS) was performed by gradient elution in methanol/water with a HP 1100 series HPLC-MS fitted with a Restek Pinnacle Cyano 5 μm (250 mm × 3.2 mm) column. Mass spectra were acquired in both positive and negative APCI and electrospray modes. Analysis for anions by ion chromatography (IC) was performed using a Dionex Bio-LC with conductivity detection and 1−100 mM OH^- gradient elution on an AS-11 column (Dionex). Infrared spectra in CCl_4 solution were acquired using a Bio-Rad FTS-45 FTIR spectrometer in transmission mode at 4 cm^{-1} resolution with a DTGS detector using a 0.1 mm path length demountable liquid cell with NaCl windows.

DRIFTS. DRIFT spectra were acquired on the same FTS-45 instrument with a liquid N_2-cooled MCT detector at 4 cm^{-1} resolution using a Spectra-Tech Collector diffuse-reflectance accessory. Solid samples were held in the diffuse reflectance accessory in the sample cup of a Spectra-Tech high temperature environmental chamber (HTEC). The sample could be resistively heated to 1000 K (±1 K), and the chamber evacuated to 1 μTorr. Gases and vapors were introduced through a separate port via a manifold. N_2 and O_2 were admitted to the manifold through separate valves after passing through a drying column as described above. DMMP vapors were admitted in reproducible amounts by first closing off the evacuated manifold and opening it to a Pyrex tube of DMMP. The Pyrex tube was then closed, and the manifold opened to the evacuated HTEC to achieve the desired DMMP pressure (typically 2 × 10^{-5} Torr per DMMP addition), Figure 1.

Prior to adsorption and photolysis experiments, 170 mg TiO_2 samples were dried in the sample cup under vacuum (~1 μTorr) at 25 °C until the broad, overlapping hydrogen-bonded TiO−H stretching vibrations from 2500 to 3800 cm^{-1} were largely removed to reveal discrete stretches in the 3400−3800 cm^{-1} region.

Irradiation of samples was carried out within the HTEC chamber and without breaking the external sample compartment purge by irradiating with a 1 kW Xe lamp (Oriel) passing through a H_2O IR filter and a 300−400 nm band-pass filter (Oriel UG-1), and focused directly into the HTEC chamber through a quartz lens mounted in the top of the sample compartment. The incident light flux on the HTEC chamber could not be measured directly but was estimated as ~100 mW cm^{-2} based on measurement of the light flux through identical optics onto a calibrated light meter (Oriel 70260 with 70282 UV Si detector). During irradiation, the sample temperature increased to as much as 70 °C, depending on the time of irradiation. Following irradiation, the sample temperature was allowed to cool to 27 °C before a spectrum was acquired.

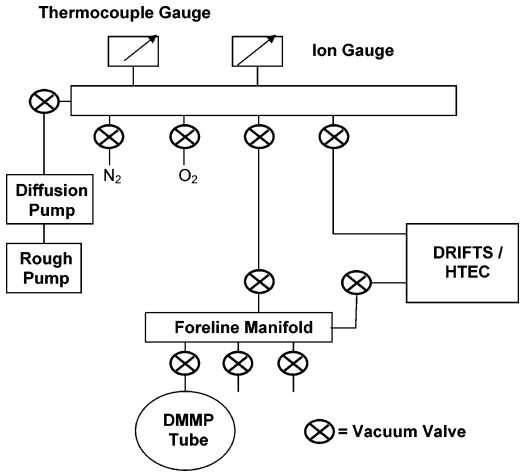

Figure 1. Schematic of vacuum system for evacuating HTEC chamber and for introducing N_2, O_2, and DMMP.

Product Analysis. The identification of gas-phase products was carried out by GC−MS analysis of the headspace gases in a static batch reactor. A powder of P-25 TiO_2 or a film of P-25 on a glass microscope slide was introduced to a 50 mL volume quartz tube reactor. Air at 50% relative humidity bubbled through DMMP at 50 °C was flowed through the reactor for 30 min. After stopping the air flow, the TiO_2 was exposed to UV irradiation from a 450 W Oriel Xe lamp which was passed through a H_2O IR filter and a 300−400 nm band-pass filter (Oriel UG-1). The light flux was 5 × 10^{19} photons s^{-1} cm^{-2} (~5 mW cm^{-2}) measured by chemical actinometry using the method of Heller and Langan.[31] Throughout the irradiation, 50 μL samples of the headspace gas were analyzed by GC−MS.

Surface-bound products from the bulk photolysis and the DRIFTS experiments were removed from the TiO_2 by washing with CH_2Cl_2, then deionized H_2O. The CH_2Cl_2 fractions were analyzed by GC−MS as described above. The water-soluble products from the CH_2Cl_2 were then extracted into H_2O, and both this H_2O fraction and the H_2O wash fraction were analyzed by LC−MS and IC.

III. Results

1. DMMP on KBr and SiO_2. For comparison with TiO_2, infrared spectra for DMMP adsorbed on nonreactive surfaces were obtained. IR data for DMMP in hexane and CCl_4 solution (transmission mode) and DMMP vapor adsorbed on KBr and SiO_2 powder (diffuse-reflectance mode) are presented in Table 1 along with band assignments. For adsorption on KBr, the IR spectrum closely matches that of DMMP in solution. On SiO_2, the IR spectrum of DMMP closely matches that of DMMP in solution, but the OH stretch band at 3728 cm^{-1} for SiO_2 disappears upon DMMP adsorption. The band assignments were obtained from normal-mode analysis of DMMP and taken from the literature.[27,32−34]

2. DMMP Adsorption at 27 °C on TiO_2. As has been observed for a number of metal oxides,[8,10,14,26,27] DMMP adsorbs

TABLE 1: DMMP IR Bands on Background Surfaces

	IR frequency (cm^{-1})			
	solution		surface adsorbed	
vibrational mode[a]	hexane[b]	CCl_4	KBr	SiO_2
$\nu_a(CH_3P)$	2992	3006	3003	3006
$\nu_a(CH_3O)$	2957	2961	2956	2961
$\nu_s(CH_3P)$	2926	2935	2925	2935
$\nu_s(CH_3O)$	2852	2857	2855	2857
$\delta_a(CH_3O)$	1467	1462	1487	
$\delta_s(CH_3O)$	1452	1448	1457	
$\delta_a(CH_3P)$	1421	1417	1423	
$\delta_s(CH_3P)$	1314	1309	1314	
ν(P═O)	1246	1251	1252	
$\rho(CH_3O)$	1185	1186	1186	
ν(CO)	1061	1066	1061	
ν(CO)	1033	1039	1040	
$\rho(CH_3P)$	914	915	917	
$\nu(PO_2)$	820	895	821	
$\nu(PO_2)$	789		794	
ν(PC)	711		712	

[a] Assignments from refs 32 and 33. [b] Values from ref 8. ν = stretch, δ = deformation, ρ = rock, s = symmetric, a = antisymmetric.

strongly on P-25 TiO_2 from the vapor phase. The adsorption process can be monitored by DRIFTS, examining the change in the spectra of both DMMP and the TiO_2 hydroxyl stretches. Upon addition of DMMP vapor to the sample chamber, bands in the 3100−2800 cm^{-1} and 1500−1000 cm^{-1} range corresponding to the IR absorptions of DMMP appear in DRIFT spectra of the TiO_2 (Figure 2 and Table 2). DMMP adsorbs specifically to surface hydroxyl groups on the TiO_2 surface as shown by the disappearance of the isolated TiO−H stretch at 3656 cm^{-1} upon addition of DMMP to a clean TiO_2 surface. New bands are observed at 3001, 2955, 2932, and 2855 cm^{-1} for DMMP (band assignments in Table 2). Additionally, a band at 2831 cm^{-1} is observed. This is assigned to the ν(Ti−OCH_3) stretch which arises from hydrolysis of the adsorbed DMMP and subsequent formation of a bound methoxy species.[27] The extent of DMMP hydrolysis upon adsorption is dependent on the surface treatment prior to DMMP adsorption and is discussed in detail below. Additional bands assigned to DMMP vibrations are observed in the range 1600−1000 cm^{-1} (Figure 2B and Table 2).

Two distinct modes of adsorption are observed for DMMP on TiO_2: dissociative and nondissociative chemisorption. This behavior was examined in detail by Rusu and Yates[27] where three distinct modes of DMMP adsorption were observed on highly dehydrated TiO_2. At temperatures below 160 K, DMMP was frozen on the outer TiO_2 surface. From 160 to 200 K DMMP migrates into the inner pores of the TiO_2 with hydrogen bonding to isolated TiOH groups and bonding to Lewis acid sites. Above 214 K DMMP adsorbs dissociatively, with formation P−OCH_3 cleavage and TiOCH_3 formation observed. The experiments reported here examine only the upper temperature regime ($T \sim 27$ °C) where adsorption proceeds with dissociation of *some* of the DMMP. The extent of dissociation is determined, in part, by the surface pretreatment of the TiO_2.

3. Effect of TiO_2 Surface Preparation on DMMP Adsorption. The method of TiO_2 surface preparation has a significant effect on the products of the DMMP adsorption process. The untreated TiO_2 surface displays a collection of broad bands at 2500−3900 cm^{-1} in the DRIFT spectra, which are due to hydrogen-bonded TiO−H stretching vibrations in different atomic environments. Sequential DRIFT spectra acquired over 14 h during dehydration of a TiO_2 sample under vacuum (~ 1 μTorr) at 27 °C are shown in Figure 3. As the surface becomes dehydrated, the broad band at 3350 cm^{-1} largely disappears, leading to peaks corresponding to discrete TiO−H stretching vibrations from 3600 to 3716 cm^{-1}.[35−37] The peak at 3416 cm^{-1} is characteristic of the rutile polymorph. These peaks in the 3300−3800 cm^{-1} range are distinct bands which are associated with O−H stretching vibrations of TiOH, $TiOH_2$, and Ti_2OH functionalities.[36]

Under dehydration conditions similar to those used by Rusu,[27] there are noticeable differences in the DRIFTS peaks for isolated

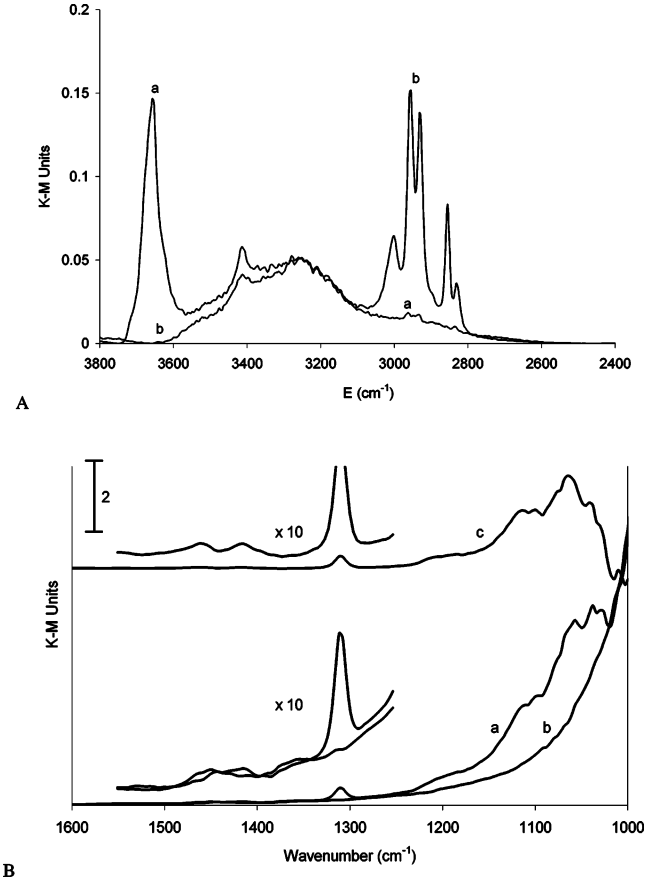

Figure 2. DRIFT spectra of P-25 TiO_2 dehydrated under vacuum 2.5 h at 150 °C and 2.5 h at 27 °C before (A) and after (B) exposure to DMMP vapor.

TABLE 2: Infrared Absorption Bands and Mode Assignments for DMMP and Ti−OCH_3

	IR frequency (cm^{-1})		
vibrational mode[a]	$DMMP_{gas}$[b]	$DMMP_{ads}$	Ti−OCH_3
$\nu_a(CH_3P)$	3014	3001	
$\nu_a(CH_3O)$	2962	2955	2929
$\nu_s(CH_3P)$	2921	2932	
$\nu_s(CH_3O)$	2859	2855	2831
$\delta_a(CH_3O)$	1471	1462	
$\delta_s(CH_3O)$		1454 sh	
$\delta_a(CH_3P)$	1423	1415	
$\delta_s(CH_3P)$	1315	1308	
$\rho(CH_3P)$	1188	1184	
ν(H_3C−O−Ti)[c]			1115
ν_s(O−P−O)[c]	1100	1099	
ν_a(C−O)	1075	1076 sh	
ν_s(C−O)	1050	1064	~1057

[a] Assignments from refs 27, 32−34. [b] Values taken from refs 33 and 34. [c] Assignment based on ref 27, see text. ν = stretch, δ = deformation, s = symmetric, a = antisymmetric.

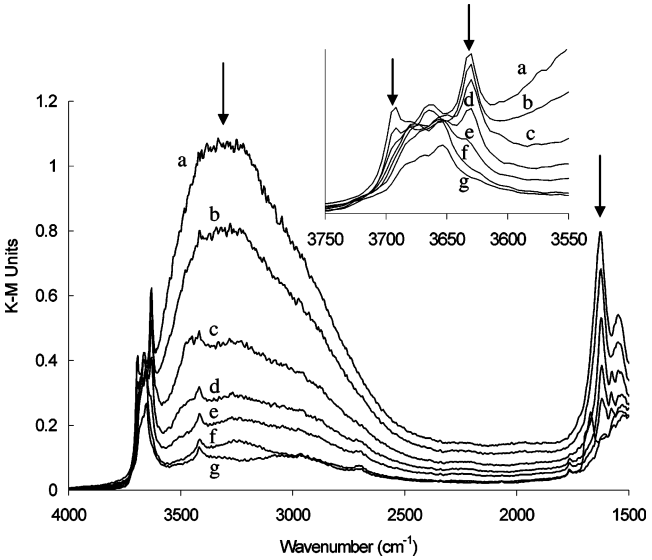

Figure 3. Vacuum dehydration of P-25 TiO_2 at RT over the course of 12 h (curves a to g in time sequence at 2 h intervals). Time = 0 is shown in curve a. Each subsequent curve (i.e., b, c, d, e, f, and g) represents a 2 h forward jump in time. Thus, for curve g, t = 12 h. The broad band at 3350 cm^{-1} due to H-bonded TiO−H stretching vibrations in different environments disappears to reveal discrete TiO−H stretches (inset).

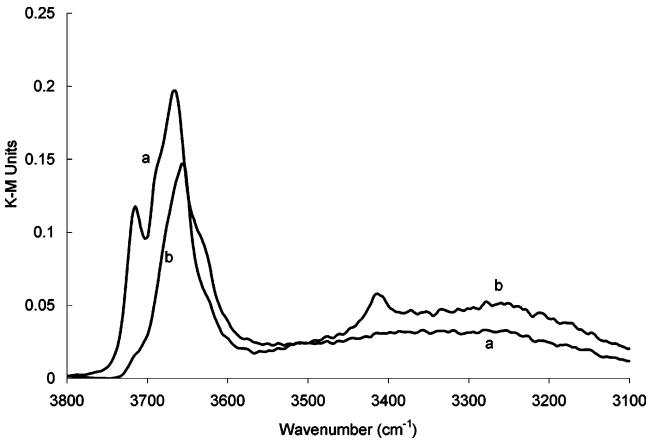

Figure 4. DRIFT spectra of TiO_2 dehydrated by heating under vacuum at 150 °C for 12 h (a) with initial irradiation for 10 min under vacuum and (b) no irradiation.

TiO−H stretching vibrations. Rusu observed five distinct bands (3728, 3722, 3678, 3664, and 3610 cm^{-1}) following 30 min at 673 K under 6 Torr O_2. By contrast, bands are observed at 3680, 3668, and 3653 cm^{-1} (Figure 2) for TiO_2 under vacuum at 27 °C for 14 h. Both these dehydration conditions and those reported by Rusu lead to DMMP degradation upon adsorption, but the extent of degradation (monitored by the ratio of the areas of the peak at 2827 cm^{-1} for Ti−OCH_3 to the peak at 2855 cm^{-1} for P−OCH_3) is greater (∼ 1:1) for Rusu's higher preparation temperature than for ours (∼1:3). The broad peak at ∼3300 cm^{-1} in Figure 2A prior to DMMP addition indicates that the TiO_2 surface still contains TiOH moieties associated with adsorbed water. This broad peak was not observed by Rusu until after DMMP was adsorbed, indicating that dissociative DMMP adsorption occurs at unassociated hydroxyl surface sites.

Broad-band UV photolysis of the surface for 10 min at the beginning of the vacuum dehydration cycle leads to results in a band at 3716 cm^{-1}, which are not observed in samples dehydrated without UV irradiation, Figure 4. The band at 3716 cm^{-1} has been previously assigned to the TiO−H stretching

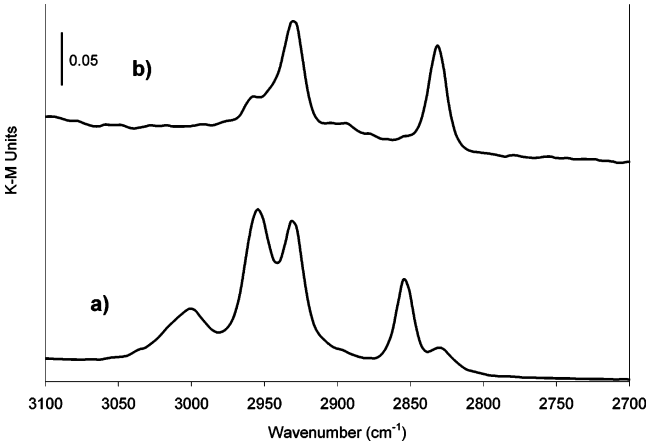

Figure 5. FTIR spectra of DMMP adsorbed on (a) preirradiated TiO_2 and (b) vacuum-dehydrated TiO_2.

vibration associated with a reduced Ti(III) surface atom resulting from a trapped electron.[37] This surface more closely resembles that of TiO_2 following 673 K preparation under O_2, where TiOH stretches at 3722 and 3726 cm^{-1} were observed.[27] The presence of the trapped electron indicated by the persistent 3716 cm^{-1} band in the photolytic surface preparation does not indicate that this is a site of direct DMMP adsorption. The increased dissociative adsorption of DMMP in samples exhibiting the 3716 cm^{-1} band is most likely a consequence of increased TiO_2 dehydration in the photolytically prepared samples. Studies on both TiO_2[27] and Al_2O_3[9,10] demonstrate DMMP chemisorption at both hydroxyl and Lewis acid sites but do not show adsorption at Lewis base sites.

For both methods of surface preparation, adsorption of DMMP results in loss of the isolated hydroxyls and re-formation of the hydrogen-bonded hydroxyls as seen by the disappearance of the 3600−3716 cm^{-1} bands, as well as appearance of bands in the 2800−3010 cm^{-1} range for DMMP methoxy C−H stretching vibrations. The bands observed in this region differ in thermally dehydrated versus photolytically/thermally dried samples. Figure 5 shows DRIFT spectra in the methyl stretching region for DMMP adsorbed on TiO_2 prepared by both methods. For the photolytically prepared sample, adsorption proceeds with a high degree of DMMP decomposition as evidenced by the dominance of the methoxy stretching region by the Ti-bound methoxy C−H stretching vibrations at 2831 and 2931 cm^{-1}. In the case of thermally prepared TiO_2, the extent of DMMP decomposition upon adsorption is greatly reduced, as shown in Figure 5b. Thermally prepared TiO_2 was used in all subsequent photooxidation studies in order to minimize the contribution of the thermal formation of $TiOCH_3$ to the photooxidation data. Following adsorption, heating the sample to 325 °C under an O_2 atmosphere does not result in a further change in the observed DRIFT spectrum.

4. Photooxidation of Adsorbed DMMP. Broad-band UV photolysis of the adsorbed DMMP leads to photooxidation and loss of the methoxy stretches in the 2800−3010 cm^{-1} region (Figures 6 and 7). Additionally, bands at 2337 and 2361 cm^{-1} increase due to the formation of CO_2 as a photooxidation product. The CO_2 bands disappear immediately upon evacuation of the HTEC chamber, even to a vacuum of $\sim 1 \times 10^{-2}$ Torr, indicating that this is gas-phase and not TiO_2-adsorbed CO_2. In contrast to Rusu and Yates,[28] no CO (2010 cm^{-1}) or formate (1586 cm^{-1}) was observed.

Gas-phase product formation during photolysis of DMMP adsorbed on TiO_2 in a static reactor was followed by GC−MS analysis throughout the course of the reaction. The gas-phase

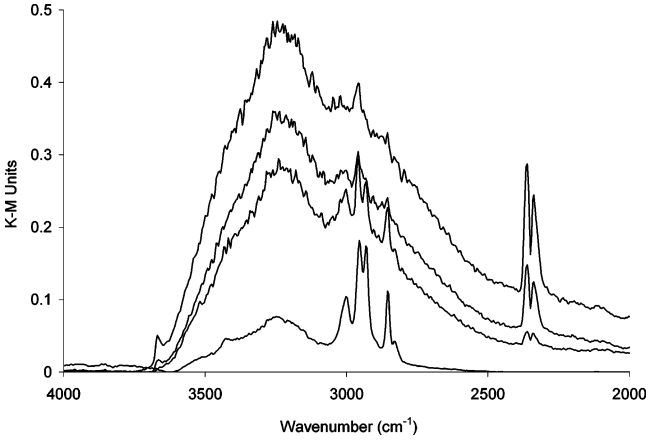

Figure 6. DRIFT spectra acquired during photolysis of DMMP on TiO_2 for 35 min. The C−H stretching vibrations between 3010 and 2800 cm^{-1} decrease with an increase in the CO_2 band at 2361 and 2337 cm^{-1}. These spectra were acquired prior to evacuation of DRIFTS cell and removal of gas-phase CO_2 produced by the photodegradation.

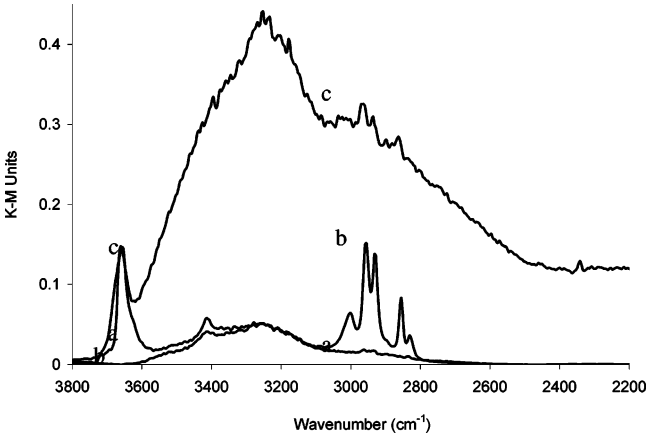

Figure 7. DRIFT spectra of DMMP photodegradation (a) showing TiO_2 prior to DMMP adsorption, (b) showing adsorbed DMMP prior to photolysis, and (c) following 35 min photolysis shown in but after evacuation of DRIFTS cell and removal of CO_2 and other gas-phase products produced by the photodegradation.

products were identical for reactions with excess DMMP directly applied to the TiO_2 surface and for DMMP adsorbed on TiO_2 from the vapor phase. Figure 8 is a plot of gas-phase product evolution. The major gas-phase constituents were DMMP, CO_2, and H_2O with trace amounts of methanol and formic acid detected. No phosphorus-containing products or intermediates (other than DMMP) were detected in the gas phase.

The production of toxic gas-phase products is a concern in systems for potential use in air purification. In this case, gas-phase methanol and formic acid are produced. Provisions would be made for recapture and continued degradation of these intermediates in a filter/photodegradation device of an actual air purification application, and the low intermediate concentrations and rapid conversion of intermediates to CO_2 should allow this to be readily accomplished.

The phosphorus-containing products of DMMP photodegradation remained adsorbed to the TiO_2 surface throughout the reaction. They were identified as methylphosphonic acid (MPA), and phosphate by IC and LC−MS analysis of organic and aqueous extractions of the TiO_2 and comparison to authentic samples of these compounds. An additional intermediate, methyl methylphosphonate (MMP), was identified by LC−MS but was not compared to an authentic sample. Kinetic simulation (discussed below), however, supports the assignment of this intermediate. For photocatalytic DMMP degradation in the static reactor, samples of the TiO_2 were removed at selected intervals and the surface-bound products and intermediates were analyzed as above. A plot of the relative distribution of products throughout the reaction is given in Figure 9.

DRIFT spectra acquired during the photodegradation of DMMP lend insight into the kinetics of the photodegradation process. DRIFTS show the loss of methoxy groups, to form MMP and MPA, then the loss of the P-bound methyl group to leave a surface-bound PO_4^{3-} species. The loss of DMMP was monitored by the decrease in the combined peak areas for the ν_{OC-H} asymmetric (2957 and 2929 cm^{-1}) and symmetric (2855 and 2827 cm^{-1}) stretching bands. The rate for the loss of P-bound methyl groups is smaller than the rate for the loss of methoxy groups: the observed decrease in the ν_{OC-H} GC peak area was exponential with an observed rate constant $k_{obs} = 0.25$ min^{-1}, and the peak area for the δ_{PC-H} bend at 1310 cm^{-1}, which is proportional to the surface concentration of DMMP, MMP, and MPA, also decreased exponentially with $k_{obs} = 0.11$ min^{-1}.

The surface-bound product (indicated by a subscript s) distribution in the static batch reactor also parallels that of the DRIFTS experiments. An initial rapid decrease in $[DMMP]_s$ leads to an increase in intermediate $[MMP]_s$ and $[MPA]_s$ followed by a slower increase in $[PO_4^{3-}]_s$. The formation of the complete mineralization product PO_4^{3-} is slow, and a high surface concentration of bound MPA remains even after long irradiation times. This is not a problem from a toxicological standpoint, however, as oxidation of DMMP to MMP in the model system corresponds to the decontamination step for organophosphorus nerve agents and pesticides. For DMMP, breaking the P−O bond in this first step is thermodynamically more difficult than breaking the P−F bond of the nerve agents GB or GD. Further degradation of MMP to PO_4^{3-} may occur more slowly and not impact the effectiveness of photodegradation as a viable chemical nerve agent destruction technique.

The final gas-phase product CO_2 is observed in the DRIFT spectra, and the peak area for CO_2 increases during the initial irradiation period. The IR bands for CO_2 at 2333 and 2360 cm^{-1} disappear immediately upon opening the HTEC to vacuum, indicating that the CO_2 is not adsorbed to the TiO_2 but is present in the gas phase. The DRIFT spectra do not show an increase in the peak for $Ti-OCH_3$ (2827 cm^{-1}) with increasing irradiation time, indicating that bound methoxy groups are not formed as observable intermediates. A small peak observed at 1568 cm^{-1} may be due to a bound formate (Ti−OOCH) intermediate. This is similar to the peak assigned to formate at 1586 cm^{-1} by Rusu et al.[28] No peaks corresponding to other C═O containing products are observed in DRIFT spectra of the irradiated TiO_2.

Data obtained from DRIFTS and product analysis lend valuable insight into the mechanism of DMMP photodegradation. The photochemical destruction of DMMP adsorbed on TiO_2 may be described by the mechanism shown in Scheme 1, a stepwise loss of CH_3OH from the phosphate core followed by a multistep oxidation of CH_3OH to CO_2. This mechanism is intended only to show the reaction pathway from DMMP to PO_4^{3-}, and it is not intended to represent the complete reaction mechanism, which would include surface species and both photochemical and thermal reactions.

A simulated degradation following this pathway is shown by the solid lines in Figure 10A. The data points in Figure 10A are obtained from ν_{OC-H} (circles) and δ_{PC-H} data. The ν_{OC-H} and δ_{PC-H} peak areas do not correspond directly to the concentrations of single species but rather to the sum of the

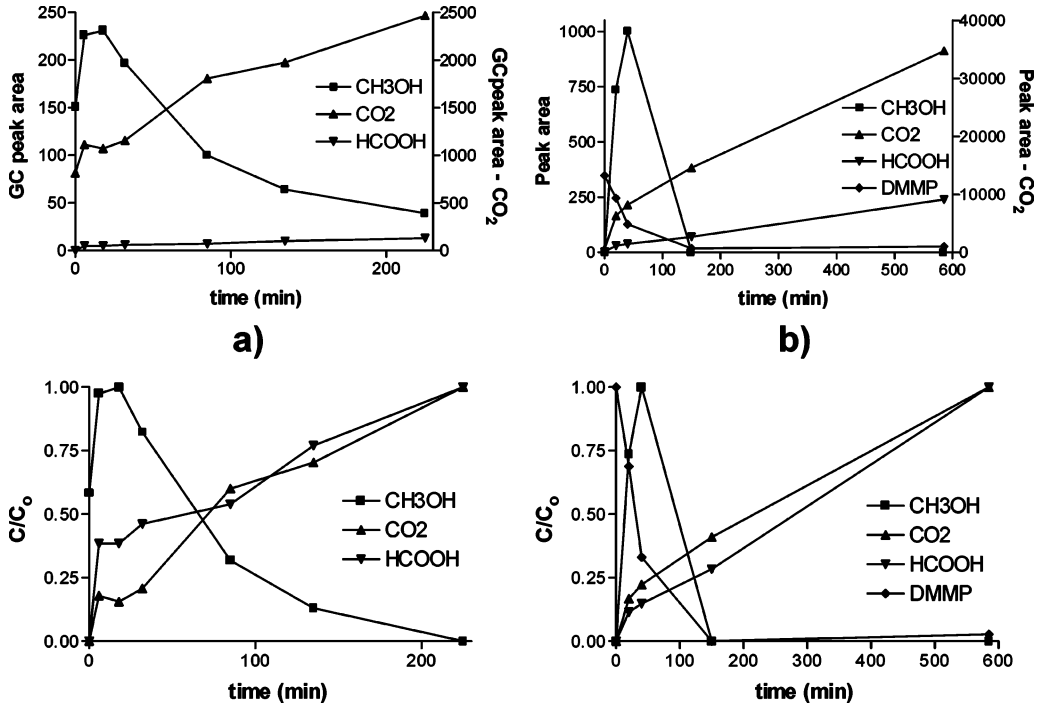

Figure 8. GC peak area and concentration versus time data for gas phase products in bulk static reactor degradation experiments: (a) heavily loaded (30 min exposure to DMMP aerosol from Collison nebulizer) and (b) lightly loaded (30 min exposure to flowing DMMP vapor at room temperature).

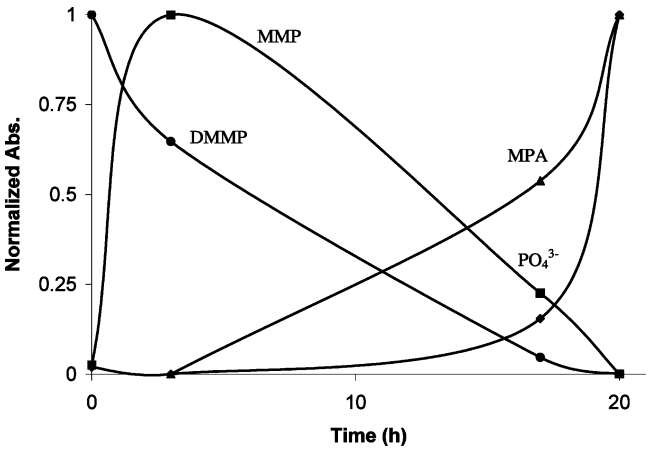

Figure 9. Surface-bound product concentration (as normalized absorbance from HPLC detector) versus time plots for photodegradation reaction products (circles = DMMP, squares = MPA, triangles = MMPA, diamonds = PO_4^{3-}) in static batch reactor with lightly loaded DMMP.

SCHEME 1

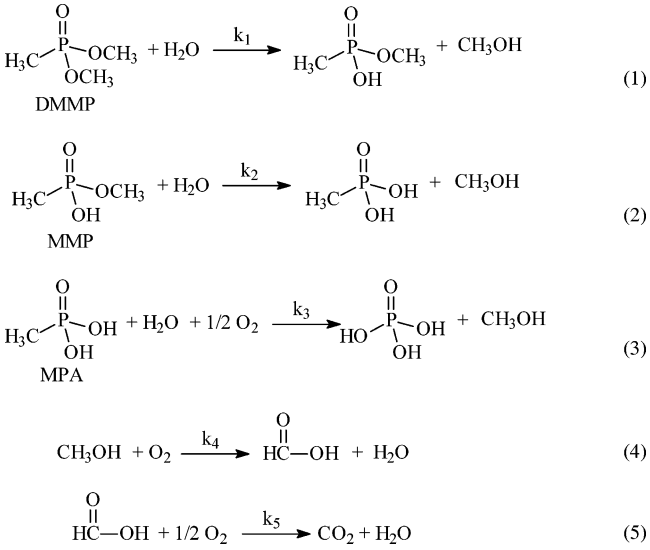

contributions from each species containing that particular vibrational mode. For [DMMP] the ν_{OC-H} data were used as obtained from the DRIFT spectra. An estimate of the time progression of [MPA] was made by subtraction of the normalized peak area for ν_{OC-H} from δ_{PC-H} (triangles). This is valid for the mechanism if $k_2 < k_3$ so that MMP will be a minor contributor to the intensity of δ_{PC-H} relative to MPA.

Similarly, reactions carried out in the static batch reactor for product analysis studies also support the mechanism shown below. Figure 10B shows the simulated normalized concentration (C/C_{max}) versus time curves for DMMP and MMP (solid lines) plotted along with data points for these two species. The presence of MMP was not identified conclusively as an intermediate as no known standard was available. LC−MS analysis of CH_2Cl_2 extractions of TiO_2 from early reaction times indicated the presence of an ion of mass 109 (negative ion ES mode) or 111 (positive ion ES). Additionally, the IC peak at earliest times, indicating an ion of −1 charge, fits the simulated kinetic profile of MMP. In the batch reactor, inhomogeneous DMMP distribution and the uncertainty of the efficiency of extraction of phosphate from TiO_2 may lead to the deviation of PO_4^{3-} formation from the mechanism above. These experiments were designed to identify possible reaction products, and the conditions were not controlled for factors affecting kinetic analysis such as light distribution and quantitative product determination. The results as obtained, however, lend support to the mechanism suggested by the DRIFT experiments and the product identity.

5. Inhibition of DMMP Photooxidation by Adsorbed Reaction Products. The inhibition of DMMP degradation by the surface-bound phosphorus-containing oxidation products was investigated by a series of DMMP loading−photodegradation

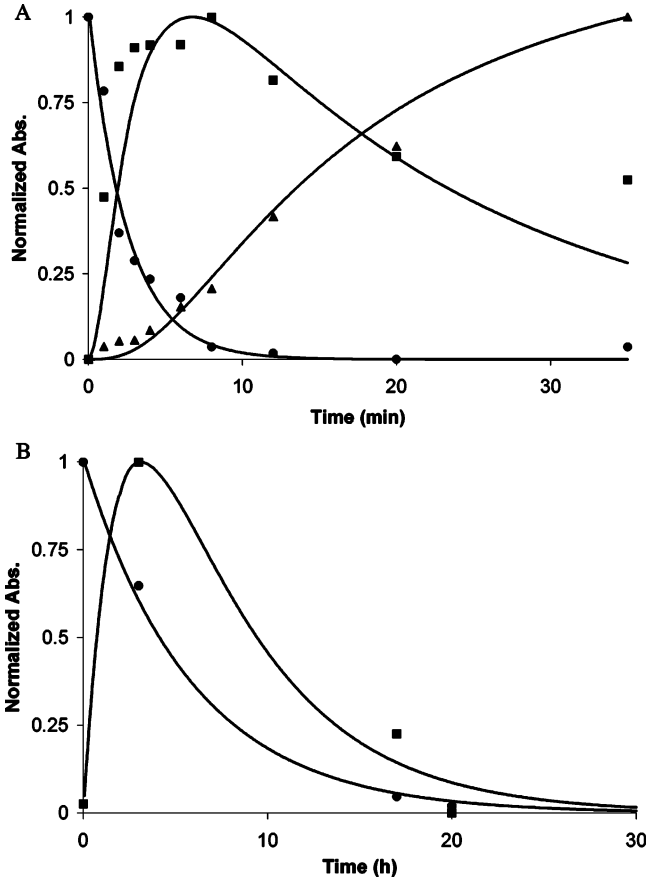

Figure 10. Simulated kinetic data for eq 1 and (A) DRIFT data for DMMP, MPA, and CO_2 and (B) static batch reactor data for DMMP and MMP.

experiments. In the DRIFTS apparatus, three successive cycles of DMMP adsorption and photooxidation were performed on the same TiO_2 sample. The MPA and PO_4^{3-} products from previous degradation reactions decrease the DMMP adsorption capacity of the TiO_2 on subsequent DMMP additions. The PO_4^{3-} and MPA products remaining bound to surface adsorption sites block further adsorption of DMMP vapor. This leads to an inhibition of photooxidation by the products of previous degradation reactions. Obee and Satyapal reported a similar inhibition, and catalytic activity of the TiO_2 could be restored by washing the surface with H_2O to remove the P-containing products.[25]

Heavy loading of DMMP on the TiO_2 surface did not inhibit photooxidation as was found by Rusu.[28] Under their conditions (190 K, 60 Torr O_2, and a more highly dehydrated surface than in this work), photooxidation is not observed for heavily loaded samples, and this is attributed to shielding of the TiO_2 sites from O_2.

Acknowledgment. Financial support of this work was provided by a grant from DARPA (through a cooperative research program with the Northrop-Grumman Corporation).

References and Notes

(1) Eckerdt, J. G.; Klabunde, K. J.; Shapley, J. R.; White, J. M.; Yates, J. T., Jr. *J. Phys. Chem. B* **1988**, *92*, 6182.

(2) Tzou, T. Z.; Weller, S. W. *J. Catal.* **1994**, *146*, 370.

(3) Baier, R. W.; Weller, S. W. *Ind. Eng. Chem. Process. Des. Dev.* **1967**, *6*, 380.

(4) Graven, W. M.; Weller, S. W.; Peters, D. L. *Ind. Eng. Chem. Process Des. Dev.* **1966**, *5*, 183.

(5) Hegde, R. I.; Greenlief, C. M.; White, J. M. *J. Phys. Chem.* **1985**, *89*, 2886.

(6) Guo, X.; Yoshinobu, J.; Yates, J. T., Jr. *J. Phys. Chem.* **1990**, *94*, 6839.

(7) Smentkowski, V. S.; Hagans, P.; Yates, J. T., Jr. *J. Phys. Chem.* **1988**, *92*, 6351.

(8) Mitchell, M. B.; Sheinker, V. N.; Mintz, E. A. *J. Phys. Chem.* **1997**, *101*, 11192.

(9) Templeton, M. K.; Weinberg, W. H. *J. Am. Chem. Soc.* **1985**, *107*, 774.

(10) Templeton, M. K.; Weinberg, W. H. *J. Am. Chem. Soc.* **1985**, *107*, 97.

(11) Henderson, M. A.; Jin, T.; White, J. M. *J. Phys. Chem.* **1986**, *90*, 4607.

(12) Barja, B. C.; Tjedor-Tjedor, M. I.; Anderson, M. A. *Langmuir* **1999**, *15*, 2316.

(13) Wagner, G. W.; Bartram, P. W.; Koper, O.; Klabunde, K. J. *J. Phys. Chem. B* **1999**, *103*, 3225.

(14) Li, Y. X.; Koper, O.; Atteya, M.; Klabunde, K. J. *Chem. Mater.* **1992**, *4*, 323.

(15) Li, Y. X.; Klabunde, K. J. *Langmuir* **1991**, *7*, 1388.

(16) Li, Y. X.; Schlup, J. R.; Klabunde, K. J. *Langmuir* **1991**, *7*, 1394.

(17) Segal, S. R.; Suib, S. L. *Chem. Mater.* **1999**, *11*, 1687.

(18) Hoffmann, M. R.; Martin, S. T.; Choi, W. Y.; Bahnemann, D. W. *Chem. Rev.* **1995**, *95*, 69.

(19) Ollis, D. W.; Al-Ekabi, H. *Photocatalytic Purification and Treatment of Water and Air*; Elsevier: Amsterdam, 1993.

(20) Serpone, N.; Pelizzetti, E. *Photocatalysis − Fundamentals and Applications*; Wiley-Interscience: New York, 1989.

(21) Ohko, Y.; Fujishima, A.; Hashimoto, K. *J. Phys. Chem. B* **1998**, *102*, 1724.

(22) Phillips, L. A.; Raupp, G. B. *J. Mol. Catal.* **1992**, *77*, 297.

(23) Lichtin, N. N.; Avudaithai, M.; Berman, E.; Dong, J. *Res. Chem. Intermed.* **1994**, *20*, 755.

(24) Dibble, L. A.; Raupp, G. B. *Catal. Lett.* **1990**, *4*, 345.

(25) Obee, T. N.; Satyapal, S. *J. Photochem. Photobiol., A* **1998**, *118*, 45.

(26) Aurian-Blajeni, B.; Boucher, M. M. *Langmuir* **1989**, *5*, 170.

(27) Rusu, C. N.; Yates, J. T., Jr. *J. Phys. Chem. B* **2000**, *104*, 12292.

(28) Rusu, C. N.; Yates, J. T., Jr. *J. Phys. Chem. B* **2000**, *104*, 12299.

(29) Barshop, B. A.; Wrenn, R. F.; Frieden, C. *Biochem. J.* **1983**, *130*, 134.

(30) Zimmerlie, C. T.; Frieden, C. *Biochem. J.* **1989**, *258*, 381.

(31) Heller, H. G.; Langan, J. R. *J. Chem. Soc., Perkin Trans. 2* **1981**, *2*, 341.

(32) Moravie, R.; Froment, F.; Corset, J. *Spectrochim. Acta* **1989**, *45A*, 1015.

(33) Van Der Veken, B.; Herman, M. *Phosphorous Sulfur* **1981**, *10*, 357.

(34) Bertilsson, L.; Engquist, I.; Liedberg, B. *J. Phys. Chem. B* **1997**, *101*, 6021.

(35) Hadjiivanov, K. I.; Klissurski, D. G. *Chem. Soc. Rev.* **1996**, *25*, 61.

(36) Contescu, C.; Popa, V. T.; Schwarz, J. A. *J. Colloid Interface Sci.* **1996**, *180*, 149.

(37) Szczepankiewicz, S. H.; Colussi, A. J.; Hoffmann, M. R. *J. Phys. Chem. B* **2001**, *104*, 9842.